FULL PAPERS

Magnetic Resonance in Medicine 52:478–484 (2004)

Highly Resolved In Vivo ^{1}H NMR Spectroscopy of the Mouse Brain at 9.4 T

Ivan Tkáč,[1] Pierre-Gilles Henry,[1] Peter Andersen,[1] C. Dirk Keene,[2,3] Walter C. Low,[2,3] and Rolf Gruetter[1,3,4]

An efficient shim system and an optimized localization sequence were used to measure in vivo ^{1}H NMR spectra from cerebral cortex, hippocampus, striatum, and cerebellum of C57BL/6 mice at 9.4 T. The combination of automatic first- and second-order shimming (FASTMAP) with strong custom-designed second-order shim coils (shim strength up to 0.04 mT/cm^2) was crucial to achieve high spectral resolution (water line width of 11–14 Hz). Requirements for second-order shim strengths to compensate field inhomogeneities in the mouse brain at 9.4 T were assessed. The achieved spectral quality (resolution, S/N, water suppression, localization performance) allowed reliable quantification of 16 brain metabolites (LCModel analysis) from 5–10-μL brain volumes. Significant regional differences (up to 2-fold, $P < 0.05$) were found for all quantified metabolites but Asp, Glc, and Gln. In contrast, ^{1}H NMR spectra measured from the striatum of C57BL/6, CBA, and CBA/BL6 mice revealed only small (<13%, $P < 0.05$) interstrain differences in Gln, Glu, Ins, Lac, NAAG, and PE. It is concluded that ^{1}H NMR spectroscopy at 9.4 T can provide precise biochemical information from distinct regions of the mouse brain noninvasively that can be used for monitoring of disease progression and treatment as well as phenotyping in transgenic mice models. Magn Reson Med 52:478–484, 2004. © 2004 Wiley-Liss, Inc.

Key words: in vivo NMR spectroscopy; shimming; mouse brain; quantification; neurochemical profile

The development of transgenic mouse models for human brain diseases represented a major advance in the investigation of the pathogenesis of several brain disorders (1–4). Because of the cost and effort involved in developing such transgenic mouse models, noninvasive methods are desirable that allow a longitudinal study design to characterize the expressed phenotype and to monitor the progress of neurodegeneration or drug treatment. In vivo NMR spectroscopy is a unique experimental technique that allows noninvasive quantification of brain metabolites. In vivo ^{1}H NMR spectroscopy has been widely used to study the brain of rats and more than 100 articles have been published (e.g., see reviews 5, 6). However, a relatively small number of studies have focused on the mouse brain (7–15). This was partly caused by the small size of the mouse brain resulting in limited signal/noise ratio (S/N). In addition, signals were broad due to the difficulties to compensate local magnetic field inhomogeneity in the small mouse head (7–13). Poor spectral resolution strongly limited the number of quantified metabolites and most of the in vivo ^{1}H NMR studies of the mouse brain to date have only reported signal intensity ratios of N-acetylaspartate, creatine, and choline (7,9,11–13,16).

Recently, it has been shown that automatic adjustment of first- and second-order shims (17,18) combined with efficient localization methods (19) can provide highly resolved in vivo ^{1}H NMR spectra at 9.4 T. The excellent spectral resolution, accurate localization, and high sensitivity resulted in the reliable quantification of more than 15 metabolites (termed "neurochemical profile") in the rat brain (20,21). Studies of brain development showed (22,23) that high-quality spectra could also be obtained from the small head of rat pups provided that the second-order shim system was strong enough to compensate nonlinear field inhomogeneities in the selected volume of interest (VOI).

As a result of the increased demands on second-order shim strength, our 9.4 T magnet was upgraded in 2001 with very strong second-order shim coils. The first aim of the present study was to demonstrate that highly spectrally and spatially resolved in vivo ^{1}H NMR spectra of the mouse brain at 9.4 T can be obtained using such shimming capabilities. A secondary aim was to determine the extent and reliability of neurochemical information that can be extracted from those spectra.

MATERIALS AND METHODS

Animals

All experiments were performed according to procedures approved by the Institutional Animal Care and Use Committee. Spontaneously breathing mice (20–25 g) were placed in a plastic chamber and anesthetized by the superfluous flow of a gas mixture containing N_2O and O_2 in a 1:1 ratio with 1.2–1.5% of isoflurane. The air temperature surrounding the mouse chamber was maintained at 30°C by warm water circulation and verified by a thermosensor. The duration of a study for a single mouse did not

[1]Center for Magnetic Resonance Research, University of Minnesota, Minneapolis, Minnesota.

[2]Department of Neurosurgery, University of Minnesota, Minneapolis, Minnesota.

[3]Graduate Program in Neuroscience, University of Minnesota, Minneapolis, Minnesota.

[4]Department of Neuroscience, University of Minnesota, Minneapolis, Minnesota.

Grant sponsor: PHS; Grant numbers: NIH P41 RR08079; F30-MH12157; Grant sponsors: W.M. Keck and Lyle French Endowment Foundations.

*Correspondence to: Ivan Tkac, Ph.D., Center for Magnetic Resonance Research, Department of Radiology, University of Minnesota, 2021 6th St. SE, Minneapolis, MN 55455. E-mail: ivan@cmrr.umn.edu

Received 22 December 2003; revised 9 April 2004; accepted 10 April 2004.

DOI 10.1002/mrm.20184

Published online in Wiley InterScience (www.interscience.wiley.com).

exceed 2 hr. The C57BL/6 mouse strain (n = 9) was used to study regional changes in concentrations of brain metabolites. In vivo ^{1}H NMR spectra from the cerebral cortex, hippocampus, striatum, and cerebellum were measured in 7, 8, 6, and 6 of these 9 mice, respectively. Two additional mouse strains (CBA, n = 5, and CBA/BL6, n = 9) were used to investigate the effect of the strain type on metabolite concentrations in a specific brain region.

^{1}H NMR Spectroscopy

All experiments were performed on a 9.4 T/31cm magnet (Magnex Scientific, Abingdon, UK) equipped with an 11 cm gradient coil (300 mT/m, 500 μs) and strong custom-designed second-order shim coils (Magnex Scientific) with maximum strengths of $XZ = 3.8 \times 10^{-2}$ mT/cm^2, $YZ = 4.5 \times 10^{-2}$ mT/cm^2, $Z^2 = 3.2 \times 10^{-2}$ mT/cm^2, $XY = 1.2 \times 10^{-2}$ mT/cm^2, $X^2Y^2 = 1.3 \times 10^{-2}$ mT/cm^2 at a current of 4 A. The magnet was interfaced to a Varian INOVA console (Varian, Palo Alto, CA). A quadrature transmit/receive surface RF coil with two geometrically decoupled single-turn coils (14 mm diameter) was used (24). All first- and second-order shim terms were automatically adjusted for each VOI using FASTMAP with EPI readout (17,18). The water signal was efficiently suppressed by variable power RF pulses with optimized relaxation delays (VAPOR) (19). Outer volume suppression (OVS) combined with the ultrashort echo-time STEAM (TE = 2 ms, TM = 20 ms, TR = 5 sec, spectral width = 5000 Hz, number of acquired complex points = 2048) was used for localization (19). The amplitudes of the crusher gradients in the STEAM sequence were increased (relative to the original version that was developed for an adult rat brain) to avoid the rephasing of unwanted magnetization during acquisition due to the highly inhomogeneous B_0 field outside the VOI. The chemical shift displacement error was minimized by using broadband RF pulses (13.5 kHz in STEAM, 35 kHz in OVS) combined with field gradients of 100–200 mT/m for slice selection. The data sampling started before the maximum of a stimulated echo (STE) to eliminate baseline distortions resulting from the incorrect amplitude of the first few data points after turning on the receiver. Those data points before STE were discarded in postprocessing. In addition, the timing of the first data point of the STE was carefully adjusted to eliminate the need for any first-order phase correction.

Driving the second-order shim coils to the maximum of their capacity resulted in a B_0 field drift up to 10 Hz/min. Similar field drifts due to insufficient heat extraction from the shim coils have been reported (25). Because real-time frequency corrections were not available on the Varian console, the drift of the resonance frequency was measured just before the data collection and then all frequencies in the pulse sequence were changed from scan to scan to follow the field drift and to remain close to an on-resonance condition. In addition, each individual FID was stored separately on disk, while maintaining the complete phase cycle. After data collection, FIDs were added in blocks of 4 or 8 (depending on S/N) and the residual frequency drift was eliminated using the signal of the methyl group of creatine. Then all blocks were summed and small residual eddy current effects were corrected using a reference water signal collected for each location. The position of the VOI was based on multislice RARE images (echo train length ETL = 8, echo spacing 15 ms, TE = 60 ms, number of phase encoding steps = 256, FOV = 20 × 20 mm, slice thickness = 1 mm, number of transients NT = 2, TR = 4 sec). ^{1}H NMR spectra were acquired from VOIs centered in the hippocampus, striatum, cerebral cortex, and cerebellum. The size of the VOI (5–10 μL) was adjusted to fit the anatomical structure of the selected brain region and to minimize partial volume effects.

Quantification

In vivo ^{1}H NMR spectra were analyzed using LCModel (26,27) as in our previous studies, which focused on the rat brain (20–23,28). The unsuppressed water signal measured from the same VOI was used as an internal reference for the quantification (assuming 80% brain water content). The LCModel analysis calculates the best fit to the experimental spectrum as a linear combination of model spectra (solution spectra of brain metabolites). The final analysis is performed in the frequency domain; however, raw data (FIDs) are used as standard data input. The following 18 metabolites were included in the basis set: alanine (Ala), aspartate (Asp), creatine (Cr), γ-aminobutyric acid (GABA), glucose (Glc), glutamate (Glu), glutamine (Gln), glutathione (GSH), glycerophosphorylcholine (GPC) phosphorylcholine (PCho), *myo*-inositol (Ins), lactate (Lac), N-acetylaspartate (NAA), N-acetylaspartylglutamate (NAAG), phosphocreatine (PCr), phosphorylehtanolamine (PE), *scyllo*-inositol, and taurine (Tau). In addition, the spectrum of macromolecules, experimentally measured in the mouse brain with an inversion recovery experiment using a short repetition time (TR = 2.0 sec, TI = 0.675 sec), was included in the basis set as previously described (20–23,28).

Statistical analysis

The SPSS software package (SPSS, Chicago, IL) was used for statistical analysis. The data for each metabolite were tested for homogeneity of variances and one-way ANOVA was used to compare the means.

RESULTS

The multislice RARE sequence provided high-quality images of the mouse brain with a spatial resolution and contrast that guaranteed precise and reproducible placement of the VOI in the hippocampus, striatum, cerebral cortex, or cerebellum (Fig. 1). In vivo ^{1}H NMR spectra from corresponding brain regions shown in Fig. 1 represent the spectral quality that was consistently achieved in this study. In addition to the commonly observed NMR signals of the methyl resonances of NAA, Cr, and Cho, characteristic spectral patterns of other metabolites, such as Ala, Asp, Glu, Gln, Ins, and Tau were discernible in ^{1}H NMR spectra from all four brain regions studied (Fig. 1). This high spectral resolution was accomplished by using FASTMAP automated shimming supported by an efficient shim system. Specifically, the availability of a very strong cus-

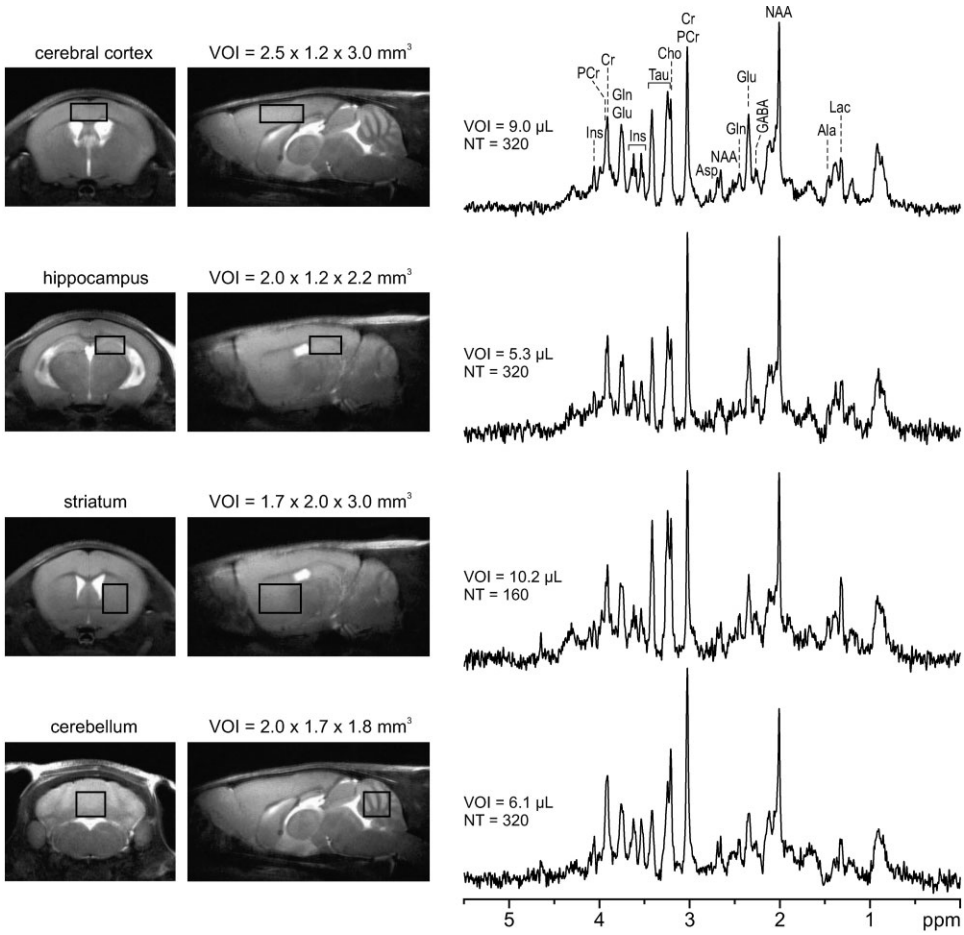

FIG. 1. Multislice RARE images of the mouse brain (C57BL/6) with the volumes of interest (VOIs) centered in cerebral cortex, hippocampus, striatum, and cerebellum and in vivo ^{1}H NMR spectra measured from the corresponding brain regions. RARE MRI: in-plane resolution 80 × 80 μm, slice thickness 1 mm, TE = 60 ms, TR = 4 sec. Localization sequence: STEAM, TE = 2 ms, TR = 5 sec, NT = 160–320, VOI = 5–10 μL. Processing: Gaussian multiplication $\{f(t) = \exp(-(t-t_{max})^2/2\sigma^2)$, $t_{max} = 0.05$ s, $\sigma = 0.085$ s$\}$, FT, zero-order phase correction. No water signal removal or baseline corrections were applied.

tom-design second-order shim coil was critical. Shimming routinely resulted in unsuppressed water signal line widths (FWHM) of 11–14 Hz.

A comparison of the average shim settings required to compensate field inhomogeneities in a particular brain region clearly demonstrated that the demands for the second-order shim strength were substantially higher in the mouse brain relative to neonatal or adult rat brain (Fig. 2a). The YZ and Z^2 shims were the most important in the hippocampus. With the exception of the Z^2 shim, where 10 out of 15 experiments requested a shim value that exceeded the maximum shim strength (shaded area), all shims were within the available shim range. In addition, a comparison of the shim requirements for different brain regions in a single mouse strain (C57BL/6) emphasized substantial spatial variation in local shims, with the highest demands on the XZ, YZ, and Z^2 shims coils (Fig. 2b). The custom-designed second-order shim coil was thus strong enough to compensate most of the field inhomogeneities in these studied regions of the mouse brain. Only the requirements for the Z^2 shim exceeded the available maximum multiple times. The averaged shim requirements to compensate the field inhomogeneities in striatum were independent of the mouse strain (data not shown).

In vivo ^{1}H NMR spectra were analyzed using LCModel and the concentrations of 16 metabolites were reliably quantified in cerebral cortex, hippocampus, striatum, and cerebellum of C57BL/6 mice (Fig. 3). Because of the strong cross-correlation between GPC and PCho arising from the close spectral similarity, only the sum of GPC and PCho was reported. The Cramer-Rao lower bounds (CRLB) corresponding to the fitted metabolites are shown in Fig. 3a,b. NAA, Glu and total creatine (Cr + PCr) were quantified with CRLB ≤ 5% from all 27 processed spectra. Another eight metabolites (Cr, PCr, GABA, Gln, Ins, Lac, Tau, GPC + PCho) were quantified with CRLB < 15% in all brain regions (Fig. 3a). Glucose and GSH were quantified with CRLB < 25% and Ala, Asp, NAAG, and PE were quantified with CRLB ranging between 15–35%. Ala and Asp were not detected in cerebellum, Ala was also not detected in striatum, and *scyllo*-inositol was not detected in all brain regions (CRLB > 50%). When expressing the CRLB in μmol/g (Fig. 3b) the estimated concentration errors were between 0.2 and 0.4 μmol/g for most of the metabolites, independent of brain region and metabolite concentration (VOI = 5–10 μL, NT = 160–320). Significant differences between the brain regions were found for nearly all brain metabolites (Fig. 3c). Metabolites such as Cr, Glu, Ins, Lac, NAA, PE, Tau, and GPC + PCho showed the largest regional variation in concentration (up to 2-fold) reaching the highest level of significance ($P < 0.0001$).

In addition to the data from C57BL/6 mice, in vivo ^{1}H NMR spectra from the striatum of CBA and CBA/BL6 mice were measured to investigate potential effects of strain type on concentrations of brain metabolites. The striatal

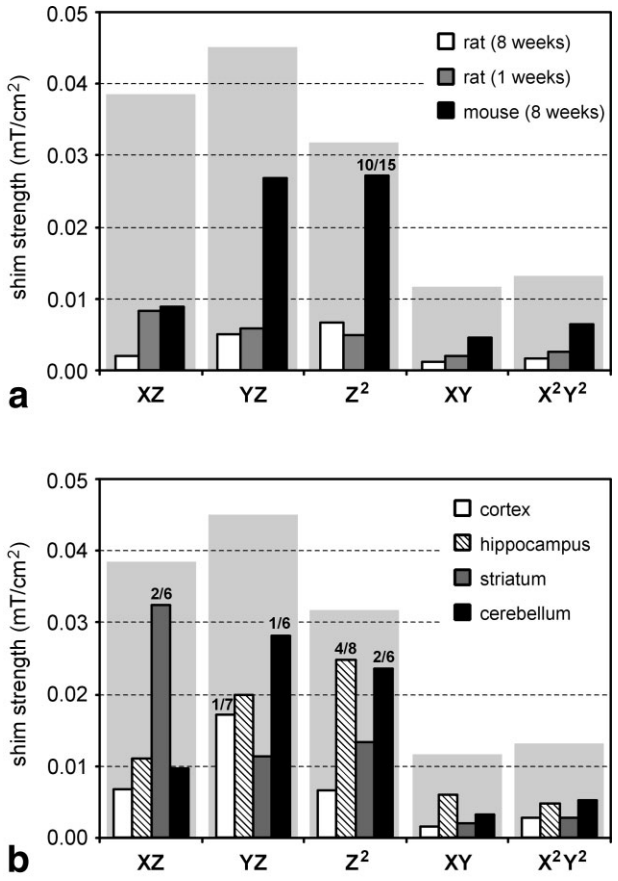

FIG. 2. Requirements for the second-order shim strengths to compensate the field inhomogeneities in the rodent brain at 9.4 T. **a:** Average shim requirements for hippocampus of adult rats (n = 25), newborn rats (n = 18), and adult mice (n = 15). Shaded areas represent available shim strength. **b:** Average shim requirements for different brain regions of C57BL/6 mice; cerebral cortex (n = 7), hippocampus (n = 8), striatum (n = 6), cerebellum (n = 6). Shaded areas represent the available shim strength. Labels on the top of bars represent the ratio of the number of cases when the requested shim values exceeded the maximum shim strength relative to the total number of studied animals.

neurochemical profiles of different mouse strains were very similar (Fig. 4). The differences in metabolite concentrations between strains did not exceed 13% and only the differences in Gln, Glu, Ins, Lac, NAAG, and PE reached the level of significance ($P < 0.05$, ANOVA).

DISCUSSION

In vivo ^{1}H NMR spectroscopy can benefit from high magnetic fields, provided that macroscopic field inhomogeneities, mostly caused by susceptibility differences between tissues and surrounding air, are minimized. The achieved spectral quality in mouse brain (Fig. 1) resulted from successful shimming up to second-order, which required an efficient B_0 mapping method and a shim system (shim coils and shim drivers) strong enough to compensate the field distortions in the VOI. In the present study, all first- and second-order shims were automatically adjusted using FASTMAP. In addition, a custom-designed second-order shim coil set was adequate to generate the required shim field strengths in most of the experiments. Demands for the second-order shim strength in the hippocampus of mice were up to 4 times higher than in the hippocampus of rats (Fig. 2a). On average, the shim strengths required for different mouse brain locations were below 0.03 mT/cm^2 for the XZ, YZ, and Z^2 coils and below 0.005 mT/cm^2 for XY and X^2Y^2 coils (Fig. 2b). Taking into account the fact that in some brain regions the required shim strengths exceeded the available maximum, the maximal strengths of all second-order shim coils should be approximately twice as high as the average shim strengths assessed experimentally (Fig. 2). Therefore, the desired shim coil should be at least 0.06 mT/cm^2 for XZ, YZ, Z^2 and at least 0.01 mT/cm^2 for XY and X^2Y^2 for spectroscopy of mouse brain at 9.4 T.

The effects of an unwanted B_0 field drift of the shim coil was minimized by incrementing all frequencies in the pulse sequence from scan to scan to follow the field drift and any residual frequency drift between spectra was eliminated by postprocessing. However, such an approach is not easily implemented for long-term averaging or CSI experiments and thus strong second-order shim coils without any field drift would be desirable.

In addition to shimming, pulse sequence performance was also important to achieve the spectral quality of this study (Fig. 1). As in our previous studies, focused on rat brain (20–23,28), the combination of STEAM with OVS guaranteed high localization performance with minimal contamination by signals from outside the VOI, such as signals from subcutaneous lipids. VAPOR water suppression was used to eliminate potential baseline distortions due to the residual water signal and permitted the reliable detection of metabolite signals in the entire chemical shift range (except for the 4.3–5.1 ppm range suppressed by VAPOR). The achieved spectral quality allowed fully automatic and operator independent data processing, which included the LCModel fitting.

The sensitivity at 9.4 T provided S/N > 10 from VOIs as small as 5–10 μL in a reasonable measuring time (15–25 min) resulting in CRLB below 20% for most of the metabolites. A high spatial resolution was required due to the small sizes of the mouse brain regions investigated (Fig. 1) and significant differences in their neurochemical profile (Fig.3c). While larger VOIs would result in better S/N, the regional specificity of the detected NMR signals would obviously be lost. In addition, larger VOIs result in reduced spectral resolution due to uncompensated third- and higher-order shim terms, which can complicate the reliable quantification of metabolites. Sensitivity can be further increased by using spin-echo based single-shot localization methods such as PRESS (29) or LASER (30), but this can typically be achieved only at the expense of increased echo time, which may result in more complicated spectral pattern and additional signal loss due to J-evolution and T_2 relaxation.

A high spectral quality (i.e., a high spectral resolution, sufficient S/N, excellent localization performance, efficient water suppression, and a distortionless baseline) was important to achieve reliable quantification of metabolite concentrations. The reliability of metabolite quantification was assessed from the average Cramer-Rao lower bounds computed by LCModel. CRLB are widely used in signal

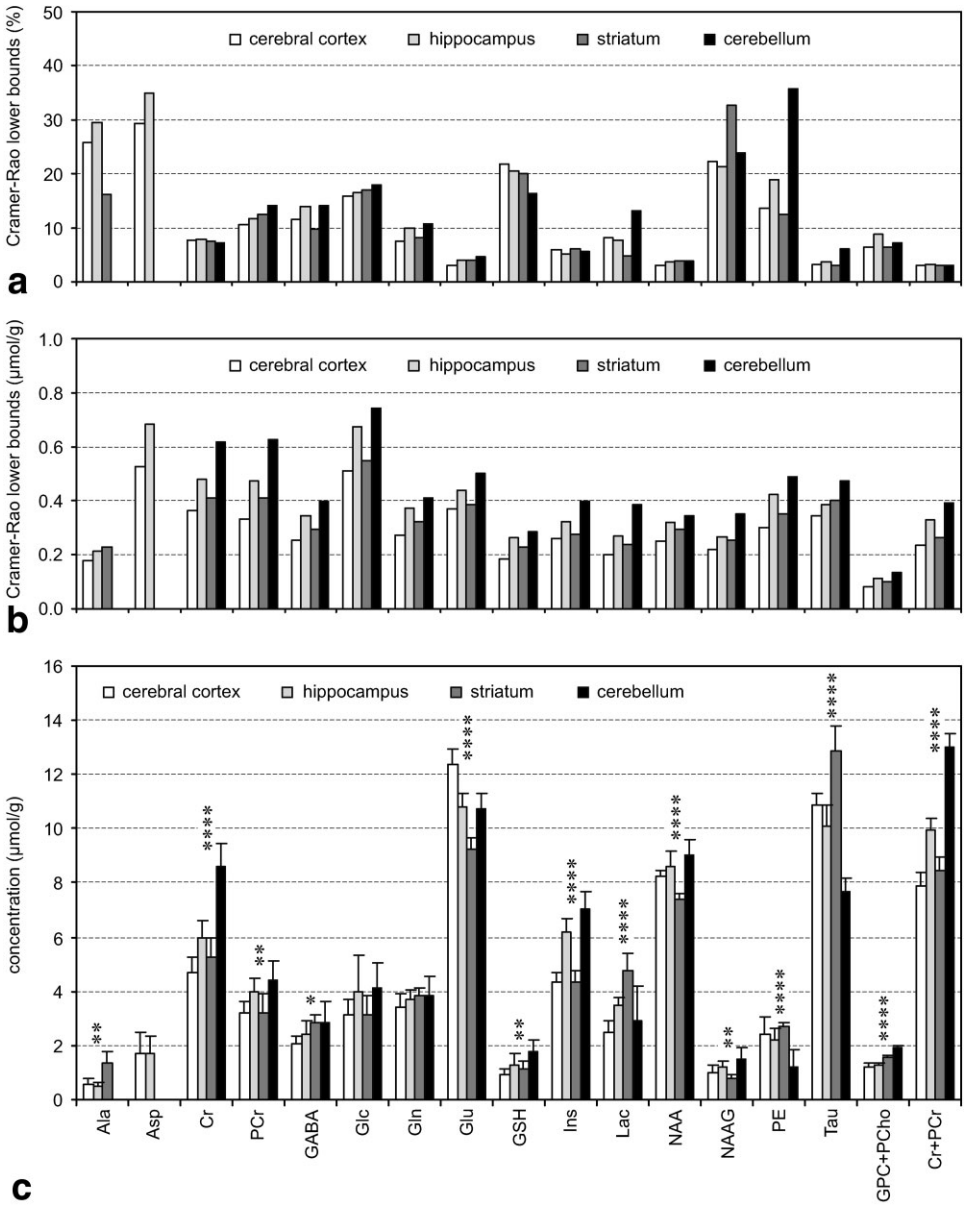

FIG. 3. Concentrations of brain metabolites and corresponding Cramer-Rao lower bound quantified by LCModel in the cerebral cortex (n = 7), hippocampus (n = 8), striatum (n = 6), and cerebellum (n = 6) of C57BL/6 mice. **a:** CRLB expressed in relative units (%). **b:** CRLB expressed in concentration units (μmol/g). **c:** Metabolite concentrations, error bars = SD. Significance level (ANOVA): $^{*}P < 0.05$, $^{**}P < 0.005$, $^{***}P < 0.0001$, $^{****}P < 0.00001$.

processing as a measure of attainable precision for the parameter estimates from a given set of observations (31). Coefficients of variation resulting from the analysis of a series of experiments were not considered as a reliable indicator for the accuracy of the metabolite quantification (32,33). CRLB, a highly important component of the standard output of the LCModel analysis (26,27), were between 3% and 20% for all mouse brain regions and for most of the metabolites (Fig. 3a). Only weakly represented metabolites of low concentration, such as Ala, Asp, NAAG, and PE, were fitted with CRLB exceeding 20%. In contrast to the CRLB (expressed in %), the CRLB expressed in concentration units (μmol/g) indicated that the absolute error was nearly independent of the metabolite concentration (Fig. 3b). This implies that the S/N ratio was the most significant factor in determining the precision of the metabolite quantification. This estimated error of metabolite quantification in the mouse brain was higher than the error (<0.2 μmol/g) reported in the developing rat brain at 9.4 T (22). This difference in precision was attributed to the lower S/N of spectra in the mouse brain relative to the rat brain (22,23) due to the smaller VOIs selected.

The comparison of metabolite concentrations in the cerebral cortex, hippocampus, striatum, and cerebellum revealed substantial and highly significant regional variations (Fig. 3c). Regional differences in the neurochemical profile were also discernible from a careful inspection of the spectra (Fig. 1). A substantially increased number of reliably quantified metabolites in the mouse brain in vivo relative to previously published data (7–15) allowed the characterization of a neurochemical profile specific and unique for each brain region (cerebral cortex, hippocampus, striatum, and cerebellum).

The brain concentration of total creatine in this study, calculated as a mean of total Cr concentration from hippocampus, striatum, and cerebral cortex, was 8.9 μmol/g.

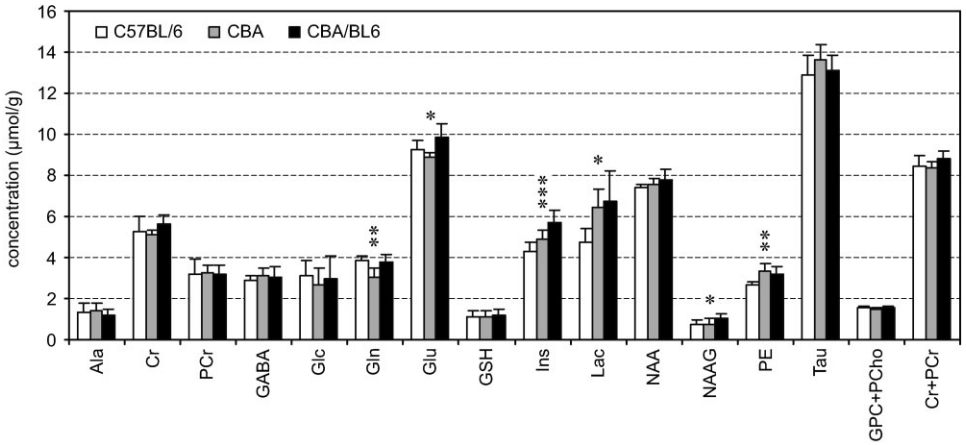

FIG. 4. Concentrations of metabolites in striatum of different mouse strains; C57BL/6 (n = 6), CBA (n = 5), CBA/BL6 (n = 9). Error bars = SD. Significance level (ANOVA): $*P < 0.05$, $**P < 0.005$, $***P < 0.0005$.

This value was in excellent agreement with the published values of 9.2 ± 1.6 mmol/L (14) and 8.2 ± 1.2 mmol/L (15). However, there are substantial differences in absolute concentrations of other metabolites such as Cho, Gln, Glu, Ins, NAA, and Tau. The differences in measured metabolite concentrations may be explained by the different spectral quality of the compared datasets, specifically the spectral resolution, as well as the differences in data processing used. The spectral quality achieved in this study, especially the high spectral resolution and S/N in spite of the very small VOIs, guaranteed low CRLB and thus reliable quantification. The CRLB of quantified metabolites (a good estimate of the reliability of the data) were not reported in the aforementioned articles (14,15). In addition, the choice of metabolites included in the basis set of LCModel and especially the incorporation of a spectrum of macromolecules for short TE spectra can also minimize systematic errors in quantification (34). For example, the unphysiologically high concentrations of Glc reported in Ref. 14 can be explained by a substantial contribution from Tau (not reported in Ref. 14), which has significant spectral overlap with glucose at 2.35 T. Comparison of the in vivo with the in vitro data from the brain extracts is difficult due to the substantial variation in reported values (12,35–37). Nevertheless, our metabolite concentrations (Fig. 3c) were in very good agreement (except NAA) with brain extract data reported by Jenkins et al. (12). In addition, the difference in neurochemical profile between cerebral cortex and striatum, e.g., higher concentrations of NAA and Tau or lower concentrations of GABA and Gln in the cortex relative to striatum, were in agreement with this earlier study (12).

Interstrain differences in metabolite concentrations were small (<13%) and limited to Gln, Glu, Ins, Lac, NAAG, and PE. A previous study has reported substantially larger differences in metabolite concentrations between other mouse strains (14). Several factors may account for these differences. For example, we noted that the shimming resulted in 3-fold broader line widths (in ppm) at 2.35 T (14) relative to our data and, in addition, line widths decreased rather than increased postmortem, which points to some difficulties with shimming. We further noted too high in vivo concentration of Glc, nonzero postmortem concentration of Glc, missing information about Tau (the metabolite with the highest concentration in the mouse brain according to our data), all pointing to systematic errors in quantification (14). In addition, the selection of large VOIs could also bias interstrain comparison, if regional metabolite variation and interstrain differences in the brain anatomy were not taken into account (38).

A close similarity in the neurochemical profiles of hippocampus, striatum, and cerebral cortex was found between mice and rats (22). For example, in the mouse brain as well as in the rat brain, Ala was always highest in striatum, Glu was highest in cortex, GSH was lowest in cortex, NAA was lowest in striatum, Ins was highest in hippocampus, Lac, Tau, and GPC + PCho were highest in striatum. These observations suggest that the pattern of the neurochemical profile may express the specifics of a given brain region across different species even though the absolute metabolite concentrations between species are distinctly different. For example, the NAA concentration was only 8 μmol/g in the cortex of mice, whereas it was 10 μmol/g in the cortex of rats, or the taurine concentration in the cortex was as high as 11 μmol/g in mice and only 8 μmol/g in rats (22). Similar to the observations in rat and mouse brain, high concentration of creatine in the cerebellum (39) and of *myo*-inositol in the hippocampus (40) relative to other brain regions were reported in humans. These observations raise the interesting possibility that the neurochemical profile reflects regional differences in function and/or neuroanatomy, in addition to the relative gray and white matter content.

We conclude that at high field, with appropriate adjustments in spectrometer hardware and experimental techniques, in vivo ^{1}H NMR spectroscopy can provide highly specific and precise biochemical information (neurochemical profile) characteristic for particular regions of the mouse brain. These experimental capabilities may allow longitudinal studies for monitoring of disease progression and treatment as well as noninvasive phenotyping in transgenic mice models.

REFERENCES

1. Bates GP, Mangiarini L, Mahal A, Davies SW. Transgenic models of Huntington's disease. Hum Mol Genet 1997;6:1633–1637.

2. Price DL, Sisodia SS, Borchelt DR. Genetic neurodegenerative diseases: the human illness and transgenic models. Science 1998;282:1079–1083.
3. Jankowsky JL, Savonenko A, Schilling G, Wang J, Xu G, Borchelt DR. Transgenic mouse models of neurodegenerative disease: opportunities for therapeutic development. Curr Neurol Neurosci Rep 2002;2:457–464.
4. Aguzzi A, Klein MA, Montrasio F, Pekarik V, Brandner S, Furukawa H, Kaser P, Rockl C, Glatzel M. Prions: pathogenesis and reverse genetics. Ann NY Acad Sci 2000;920:140–157.
5. Hoehn M, Nicolay K, Franke C, van der Sanden B. Application of magnetic resonance to animal models of cerebral ischemia. J Magn Reson Imag 2001;14:491–509.
6. Choi IY, Lee SP, Guilfoyle DN, Helpern JA. In vivo NMR studies of neurodegenerative diseases in transgenic and rodent models. Neurochem Res 2003;28:987–1001.
7. Tracey I, Dunn JF, Parkes HG, Radda GK. An in vivo and in vitro H-magnetic resonance spectroscopy study of mdx mouse brain: abnormal development or neural necrosis? J Neurol Sci 1996;141:13–18.
8. Hesselbarth D, Franke C, Hata R, Brinker G, Hoehn-Berlage M. High resolution MRI and MRS: a feasibility study for the investigation of focal cerebral ischemia in mice. NMR Biomed 1998;11:423–429.
9. Huang W, Galdzicki Z, van Gelderen P, Balbo A, Chikhale EG, Schapiro MB, Rapoport SI. Brain myo-inositol level is elevated in Ts65Dn mouse and reduced after lithium treatment. Neuroreport 2000;11:445–448.
10. van Dellen A, Welch J, Dixon RM, Cordery P, York D, Styles P, Blakemore C, Hannan AJ. N-Acetylaspartate and DARPP-32 levels decrease in the corpus striatum of Huntington's disease mice. Neuroreport 2000; 11:3751–3757.
11. Matalon R, Rady PL, Platt KA, Skinner HB, Quast MJ, Campbell GA, Matalon K, Ceci JD, Tyring SK, Nehls M, Surendran S, Wei J, Ezell EL, Szucs S. Knock-out mouse for Canavan disease: a model for gene transfer to the central nervous system. J Gene Med 2000;2:165–175.
12. Jenkins BG, Klivenyi P, Kustermann E, Andreassen OA, Ferrante RJ, Rosen BR, Beal MF. Nonlinear decrease over time in N-acetyl aspartate levels in the absence of neuronal loss and increases in glutamine and glucose in transgenic Huntington's disease mice. J Neurochem 2000; 74:2108–2119.
13. Andreassen OA, Jenkins BG, Dedeoglu A, Ferrante KL, Bogdanov MB, Kaddurah-Daouk R, Beal MF. Increases in cortical glutamate concentrations in transgenic amyotrophic lateral sclerosis mice are attenuated by creatine supplementation. J Neurochem 2001;77:383–390.
14. Schwarcz A, Natt O, Watanabe T, Boretius S, Frahm J, Michaelis T. Localized proton MRS of cerebral metabolite profiles in different mouse strains. Magn Reson Med 2003;49:822–827.
15. Renema WK, Schmidt A, van Asten JJ, Oerlemans F, Ullrich K, Wieringa B, Isbrandt D, Heerschap A. MR spectroscopy of muscle and brain in guanidinoacetate methyltransferase (GAMT)-deficient mice: validation of an animal model to study creatine deficiency. Magn Reson Med 2003;50:936–943.
16. Andreassen OA, Dedeoglu A, Ferrante RJ, Jenkins BG, Ferrante KL, Thomas M, Friedlich A, Browne SE, Schilling G, Borchelt DR, Hersch SM, Ross CA, Beal MF. Creatine increases survival and delays motor symptoms in a transgenic animal model of Huntington's disease. Neurobiol Dis 2001;8:479–491.
17. Gruetter R. Automatic, localized in vivo adjustment of all first- and second-order shim coils. Magn Reson Med 1993;29:804–811.
18. Gruetter R, Tkac I. Field mapping without reference scan using asymmetric echo-planar techniques. Magn Reson Med 2000;43:319–323.
19. Tkac I, Starcuk Z, Choi IY, Gruetter R. In vivo 1H NMR spectroscopy of rat brain at 1 ms echo time. Magn Reson Med 1999;41:649–656.
20. Pfeuffer J, Tkac I, Provencher SW, Gruetter R. Toward an in vivo neurochemical profile: quantification of 18 metabolites in short-echo-time (1)H NMR spectra of the rat brain. J Magn Reson 1999;141:104–120.
21. Tkac I, Keene CD, Pfeuffer J, Low WC, Gruetter R. Metabolic changes in quinolinic acid-lesioned rat striatum detected non-invasively by in vivo (1)H NMR spectroscopy. J Neurosci Res 2001;66:891–898.
22. Tkac I, Rao R, Georgieff MK, Gruetter R. Developmental and regional changes in the neurochemical profile of the rat brain determined by in vivo 1H NMR spectroscopy. Magn Reson Med 2003;50:24–32.
23. Rao R, Tkac I, Townsend EL, Gruetter R, Georgieff MK. Perinatal iron deficiency alters the neurochemical profile of the developing rat hippocampus. J Nutr 2003;133:3215–3221.
24. Adriany G, Gruetter R. A half-volume coil for efficient proton decoupling in humans at 4 Tesla. J Magn Reson 1997;125:178–184.
25. Henry PG, van de Moortele PF, Giacomini E, Nauerth A, Bloch G. Field-frequency locked in vivo proton MRS on a whole-body spectrometer. Magn Reson Med 1999;42:636–642.
26. Provencher SW. Estimation of metabolite concentrations from localized in vivo proton NMR spectra. Magn Reson Med 1993;30:672–679.
27. Provencher SW. Automatic quantitation of localized in vivo 1H spectra with LCModel. NMR Biomed 2001;14:260–264.
28. Pfeuffer J, Tkac I, Gruetter R. Extracellular-intracellular distribution of glucose and lactate in the rat brain assessed noninvasively by diffusion-weighted 1H nuclear magnetic resonance spectroscopy in vivo. J Cereb Blood Flow Metab 2000;20:736–746.
29. Bottomley PA. Spatial localization in NMR spectroscopy in vivo. Ann NY Acad Sci 1987;508:333–348.
30. Garwood M, DelaBarre L. The return of the frequency sweep: designing adiabatic pulses for contemporary NMR. J Magn Reson 2001;153:155–177.
31. Cavassila S, Deval S, Huegen C, van Ormondt D, Graveron-Demilly D. Cramer-Rao bounds: an evaluation tool for quantitation. NMR Biomed 2001;14:278–283.
32. Tkac I, Kim J, Ugurbil K, Gruetter R. Quantification of 7 Tesla 1H NMR spectra of the human brain using LCModel and spin simulation. In: Proc ISMRM/ESMRMB Meeting, Glasgow, 2001.
33. Kreis R, Boesch C. Bad spectra can be better than good spectra. In: Proc 11th Annual Meeting ISMRM, Toronto, 2003.
34. Hofmann L, Slotboom J, Jung B, Maloca P, Boesch C, Kreis R. Quantitative 1H-magnetic resonance spectroscopy of human brain: Influence of composition and parameterization of the basis set in linear combination model-fitting. Magn Reson Med 2002;48:440–453.
35. Le Moyec L, Ekwalanga M, Eugene M, Bouanga JC, Bauza G, M'Bengue A, Mazier D, Gentilini M. Brain metabolites in mice coinfected with Plasmodium berghei ANKA and LP-BM5 virus: assessment by proton magnetic resonance spectroscopy. Exp Parasitol 1997;85:296–298.
36. Tsao JW, Paramananthan N, Parkes HG, Dunn JF. Altered brain metabolism in the C57BL/Wld mouse strain detected by magnetic resonance spectroscopy: association with delayed Wallerian degeneration? J Neurol Sci 1999;168:1–12.
37. Yao FS, Caserta MT, Wyrwicz AM. In vitro proton and phosphorus NMR spectroscopic analysis of murine (C57Bl/6J) brain development. NMR Biomed 1999;12:463–470.
38. Beckmann N. High resolution magnetic resonance angiography noninvasively reveals mouse strain differences in the cerebrovascular anatomy in vivo. Magn Reson Med 2000;44:252–258.
39. Pouwels PJ, Frahm J. Regional metabolite concentrations in human brain as determined by quantitative localized proton MRS. Magn Reson Med 1998;39:53–60.
40. Kassem MN, Bartha R. Quantitative proton short-echo-time LASER spectroscopy of normal human white matter and hippocampus at 4 Tesla incorporating macromolecule subtraction. Magn Reson Med 2003;49:918–927.